ORIGINAL PAPER

Oxygen isotopic compositions of meteoric precipitation, drip water, and aragonitic stalagmite deposition from the Namjang cave in northwestern Thailand: implications for multi-proxy climate reconstruction

Chotika Muangsong[1] · Nathsuda Pumijumnong[2] · Binggui Cai[3,4] · Chaoyong Hu[5]

Abstract

Stalagmites provide one of the few high-quality proxy records of the Thailand monsoon. The Namjang (NJ) cave (19°40′30″N, 98°12′12″E; 923 m a.s.l.), which is situated in the data-scarce region of northwestern Thailand, serves as a unique and important site that offers great potential for multi-proxy climate reconstruction. We present new data on stable oxygen isotopic (δ^{18}O) compositions and growth rates of aragonite stalagmites based on an in situ cave and climate monitoring study performed between August 2012 and October 2013. The dominant factors that control the variations in the δ^{18}O values of rainfall, drip water, and modern aragonite precipitate as well as the variations in the modern speleothem deposition rates and drip water hydrochemical properties were determined to correctly interpret the climatic signals of the parameters that are derived from speleothems. The intraseasonal variations in rainfall δ^{18}O values were faithfully recorded from cave drip water isotopic signals. The monthly mean values of δ^{18}O in cave drip water were lower in the rainy season and higher in the dry seasons and shifted from approximately − 4 in the early rainy months to approximately − 6‰ in the late rainy months. These variations have implications for the use of speleothem δ^{18}O from the NJ cave as a proxy of the seasonal variations in monsoon rainfall δ^{18}O and changes in moisture source trajectories. The deposition rates of modern speleothem deposits are primarily controlled by drip water flow rates, which are linked to the amount of water recharge in the cave during the summer monsoon season. There was a significant correlation between the drip rate and amount of carbonate precipitation for the drip sites NJ-1 ($r = 0.54$, $p < 0.040$) and NJ-1202 ($r = 0.76$, $p < 0.004$). Combinations of different parameters and proxies from this area could provide the potential for the further development of multi-proxy climate reconstructions over different time scales.

✉ Nathsuda Pumijumnong
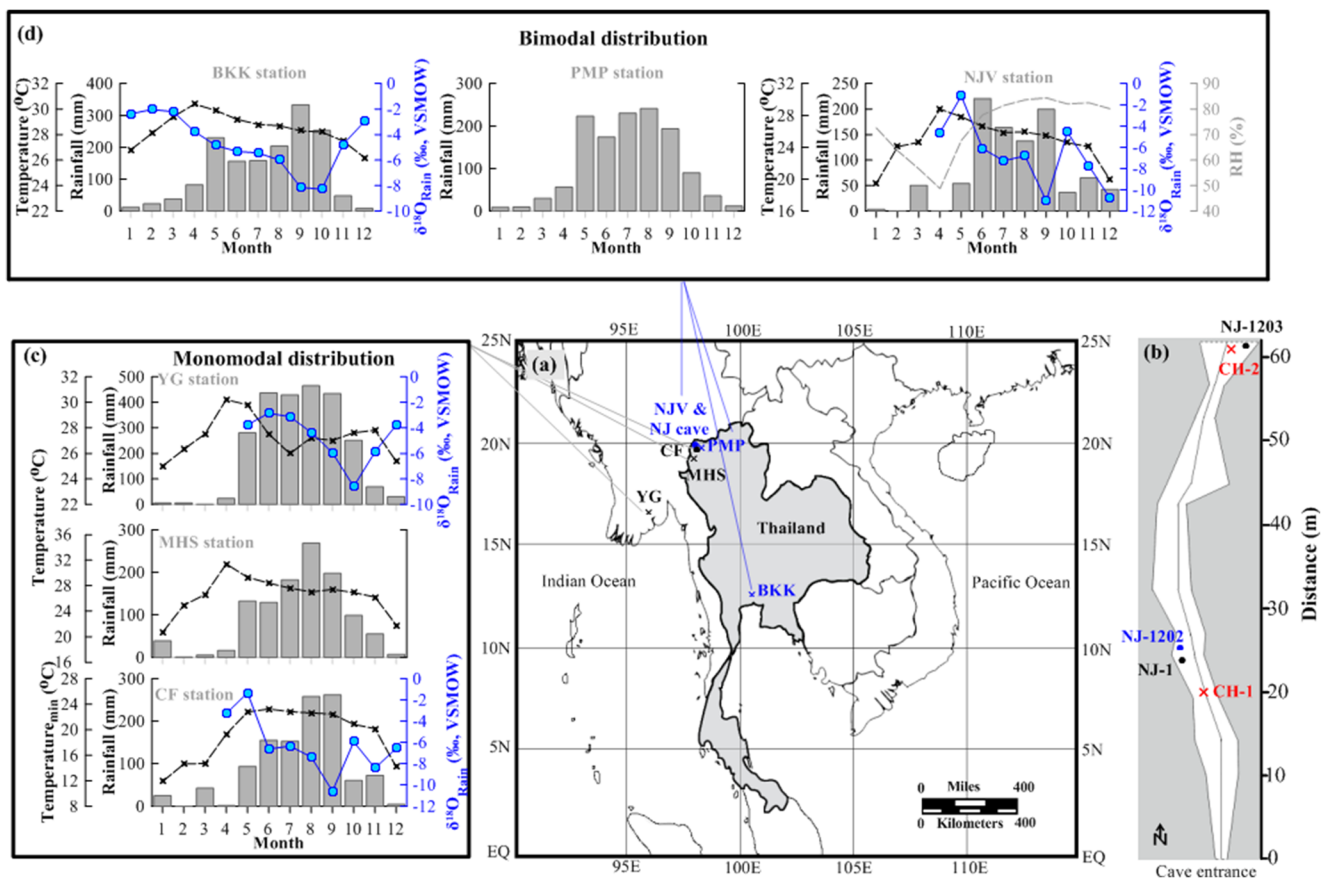nathsuda@gmail.com; nathsuda.pum@mahidol.ac.th

1   Innovation for Social and Environmental Management, Mahidol University, Amnatcharoen campus, Amnatcharoen 37000, Thailand

2   Faculty of Environment and Resource Studies, Mahidol University, Nakhon Pathom 73170, Thailand

3   Key Laboratory for Humid Subtropical Eco-geographical Processes of the Ministry of Education, Fujian Normal University, Fuzhou 350007, China

4   Institute of Geography, Fujian Normal University, Fuzhou 350007, China

5   State Key Laboratory of Biogeology and Environmental Geology, China University of Geosciences, Wuhan 430074, China

1 Introduction

Monsoon rainfall provides a vital supply of water for most Asian monsoon countries. Tropical and subtropical regions, where the vast amount of atmospheric moisture originates in this region, are of particular interest for paleoclimate studies (Cobb et al. 2007; Lewis et al. 2010). Thailand is a country in Southeast Asia (Fig. 1a). Thailand monsoon (TM) is regarded as a tropical monsoon climate and is located in a transition zone between the Indian monsoon (IM) and western North Pacific (WNP) monsoon (WNPM) (Wang and Ho 2002; Wei et al. 2018). The stable oxygen isotopic (δ^{18}O) signature of water is an important tracer for hydrological and ecological processes (Clark and Fritz 1997; West et al. 2006; Kumar et al. 2010). Among many applications, δ^{18}O and δD have been used extensively to determine the origin and pathway of atmospheric water vapor (Srivastava et al. 2015) and to interpret

Fig. 1 **a** Map of the study region highlighting the location of the Namjang cave (NJ) (19°40′30″N, 98°12′12″E); two monitoring stations, including the Namjang village (NJV) station (19°40′5″N, 98°12′13″E, AD 2012–2013) and Baan Café Nature Resort (CF) station (19°31′8″N, 98°14′51″E, AD 2012–2013), and the meteorological station in the regions. **b** Plan view of the Namjang cave (modified from Phutong 2008) showing the location of drip sampling sites (NJ-1, NJ-1202, and NJ-1203) and cave microclimate monitoring location (CH-1 and CH-2). **c–d** Climate data of the study region including the monthly average rainfall (gray vertical bar), temperature (black dashed line with asterisk), relative humidity (gray dashed line), and rainfall δ^{18}O value (solid line with solid blue circles) at the two monitoring stations (NJV and CF) in this study, Mae Hong Son (MHS 19°18′N, 97°50′E, AD 1911–2013) and Pang Ma Pha (PMP 19°31′N, 98°15′E, AD 1987–2013) meteorological stations (Thai Meteorological Department, 2013) as well as Bangkok (BKK 13°44′N, 100°34′E, AD 1968–2004) and Yangon (YG 16°46′N, 96°10′E, AD 1961–1963) stations (IAEA/WMO 2001)

paleoclimate proxies (Cobb et al. 2007). However, the main factors that control the isotopic composition in rainfall at any given site in a tropical area remain debatable because there is a combination of numerous factors that influence oxygen isotopes in meteoric water (i.e., rainfall), and these factors sometimes operate strictly locally rather than regionally (Dansgaard 1964; Araguás-Araguás et al. 1998; Aggarwal et al. 2004; Lewis et al. 2010; Wei et al. 2018). A better understanding of the hydrology and isotopic chemistry of tropical monsoon rainfall are of great importance for paleoclimate reconstruction, especially in countries located in the boundary area among the different monsoon regions.

The Namjang (NJ) cave (19°40′30″N, 98°12′12″E) (Fig. 1b) (located in a western region of the Pang Ma Pha (PMP) district in Mae Hong Son (MHS) province of northwestern (NW) Thailand) is situated in a climate-sensitive area under the influence of the Asian monsoon climate and is ideally suited for paleomonsoon studies (Cai et al. 2010;

Muangsong et al. 2011, 2014, 2016, 2018). The tropical climate in this area is characterized by dry (winter and summer) and wet (rainy) seasons. Paleoclimate records from this region are mainly derived from tree rings (Buckley et al. 2007; Pumijumnong and Eckstein 2011; Buajan et al. 2016; Muangsong et al. 2016, 2018, 2020; Payomrat et al. 2018; Pumijumnong et al. 2020) and stalagmites (Cai et al. 2010; Muangsong et al. 2011, 2014; Chawchai et al. 2018). Although the variability of speleothem δ^{18}O from tropical and subtropical regions is largely interpreted as being representative of the rainfall amount (Yadava et al. 2004; Lewis et al. 2011; Denniston et al. 2013), this explanation is under debate due to the other factors that influence rainfall δ^{18}O at a specific site that may not be related to the rainfall amount (Fischer and Treble 2008). In this area, the interpretation of proxy records is complicated due to the seasonal response to the seasonal surface climate (Cai et al. 2010; Muangsong et al. 2011, 2014, 2016, 2018). Previous studies emphasized the key

effect of seasonal monsoon rainfall on either the $\delta^{18}O$ values or growth rates of stalagmites and tree ring proxies rather than total rainfall (Cai et al. 2010; Muangsong et al. 2011, 2014, 2016, 2018). In addition to several factors that contribute to the variation of oxygen isotopes in rainfall, water movement processes in the soil zone and epikarst, as well as carbonate precipitation processes, may modify the signal to different degrees before it is incorporated into speleothems (Fairchild et al. 2006; Lachniet 2009). Currently, there is a significant gap in studies on speleothem-based climate proxy data in tropical and subtropical regions due to the lack of detailed cave and climate conditions that can delineate factors that control speleothem properties. Monitoring data of cave and climate systems are essential to correctly interpret the paleoclimate signals that are preserved in stalagmites in this area.

We present new data on the oxygen isotopic compositions and growth rates of aragonite stalagmites from the NJ cave in MHS province of NW Thailand based on cave and climate monitoring data collected between August 2012 and October 2013. The data provide the first results of the constraining factors that affect Thai stalagmite parameters, and demonstrate the potential use of stalagmites for a multi-proxy reconstruction of the Thailand monsoon.

2 Study area and climatology

The NJ cave (19°40′30″N, 98°12′12″E; 923 m a.s.l.) (Fig. 1 a and b) is located in a western region of the PMP district in the MHS province of NW Thailand (Cai et al. 2010; Muangsong et al. 2016). The cave developed in Permian limestone and a dolostone formation. The NJ cave is approximately 6-m wide and 60-m long with one narrow entrance (Phutong 2008) (Fig. 1b). The overlying bedrock is approximately 5 m in depth (Phutong 2008). XRD analysis indicated that the investigated stalagmite samples were aragonite (Phutong 2008; Cai et al. 2010). The natural vegetation covering this site consists of mixed deciduous forest with teak (*Tectona grandis* L.) (Muangsong et al. 2018).

Typically, the three seasons of winter (November to the next February), summer (March to April), and rainy (May to October) are dominated by two monsoon regimes, namely the southwest (SW) monsoon (or summer monsoon) and northeast (NE) monsoon (or winter monsoon). According to the climate data obtained from the MHS (located approximately 45 km from the cave) and PMP (located approximately 19 km from the cave) local meteorological stations between AD 1911 and 2013 (Thailand Meteorological Department 2013), more than 90% of the annual precipitation falls during the SW monsoon (rainy season) from May to October (Fig. 1 c and d). The rainy season is generally divided into two rainy seasons, namely, the early (May–June–July; hereafter referred to as MJJ rainfall) and late (August–September–October; hereafter

referred to as ASO rainfall) rainy seasons (Cai et al. 2010; Muangsong et al. 2016, 2018). The available data from the MHS station show that the mean monthly temperature (T) is 30 °C in summer, while the temperatures can drop to as low as 22 °C in winter (Thailand Meteorological Department 2013). Heterogeneous distribution of rainfall can be observed in Thailand even at the meteorological stations that are only a few kilometers apart (Kuenzer 2014). The climate of the study region is described in detail in previous studies (Cai et al. 2010; Muangsong et al. 2016, 2018).

3 Materials and methods

3.1 Local atmospheric climate and cave air climate monitoring

Local atmospheric climate and cave air climate monitoring were conducted between August 2012 and October 2013. Atmospheric climate variables, including temperature, relative humidity (RH), and rainfall amount, were monitored both at the Namjang village (NJV) and the Baan Café Nature Resort (CF) stations (Fig. 1a). The NJV station (19°40′5″N, 98°12′13″E; 900 m a.s.l.) is approximately 1 km from NJ cave, while the CF station (19°31′8″N, 98°14′51″E; 800 m a.s.l.) is located in the town of PMP which is approximately 30 km from the NJ cave (Fig. 1a).

The cave air microclimate conditions (T and RH) were monitored approximately 20 m from the cave entrance (hereafter referred to as "CH-1"), as well as in the inner chamber approximately 60 m from the cave entrance (hereafter referred to as "CH-2") (Fig. 1b). The air temperature and relative humidity were measured by the Onset HOBO® data logger (Onset Corporation, Bourne, MA, USA), except for the temperature at the CF station, which was measured by a manual Thermometer at 7 am every day (hereafter referred to as "minimum temperature or temperature$_{min}$") (Thailand meteorological department 2013). Unfortunately, we did not have monitoring equipment on cave air's carbon dioxide (CO_2) during the study period between AD 2012 and 2013. The only available cave air CO_2 data from the NJ cave were those collected during cave visit on May 5, 2018 using the Onset HOBO® MX1102 Bluetooth (BLE) CO_2 data logger (Onset Corporation, Bourne, MA, USA). The amount of local rainfall was automatically recorded by the Onset HOBO® RG3 data logging rain gauge (Onset Corporation, Bourne, MA, USA) at the NJV station. The amount of local rainfall was manually measured with a traditional rain gauge at the CF station. In both sites, the cumulative monthly rainfall was collected using a clean plastic container covered by aluminized paper to block sunshine. At each collection, paraffin oil was placed in the empty container in advance to prevent evaporation. A water sample for measuring stable isotopes

was subsampled and preserved in an amber glass vial, which was then sealed by parafilm.

3.2 Drip water hydrochemical monitoring

A total of three drip sites in the NJ cave were selected in this study, including a site to measure the drip water that feeds the previously studied stalagmite NJ-1 (Cai et al. 2010; Muangsong et al. 2011) (hereafter referred to as the "NJ-1" drip sampling site) and an additional two drip sites located near the location of NJ-1 (hereafter referred to as the "NJ-1202" drip sampling site) and in the inner chamber (hereafter referred to as the "NJ-1203" drip sampling site) (Fig. 1b). Accumulated drip water samples were collected on monthly to seasonal time scales, and instantaneous (or actual) drip water samples were collected during the field trip. At each site, the drip rate and hardness level were measured. Drip water was also sampled and preserved in an amber glass vial for stable isotope analysis. To determine the carbonate precipitation rate of drip water, a glass substrate (10 x 10-cm plates) was placed beneath each drip and was retrieved every month. The drip rates were defined by counting the number of drops per unit time. The hardness level was determined according to the calcium carbonate ($CaCO_3$) concentration, which was measured using the Aquamerck® carbonate hardness test kit (Merck Company, German). Selected hydrochemistry properties of cave drip water, e.g., electrical conductivity (EC) and pH were measured using portable pH and EC meters. The amount of aragonite precipitates, which represents the stalagmite growth rate or deposition rate, was measured by weighing the amount of aragonite precipitated on the glass plates. Powder subsamples of the aragonite precipitate were then scraped from the center of the glass plate to measure the isotopic ratio.

3.3 Stable isotopic ratio measurement

The stable isotope ratios (δD and $\delta^{18}O$) from water samples, both of rain and drip waters, were analyzed at the State Key Laboratory of Hydrology-Water Resources and Hydraulic Engineering, Hehai University, China, using a MAT-253 stable isotope ratio mass spectrometer (Thermo Electron Corporation, Brement, Germany), as well as at the State Key Laboratory of Biogeology and Environmental Geology, China University of Geosciences (Wuhan), using a liquid water isotope analyzer (IWA-35-EP, LGR). The precision was 0.1‰ for both $\delta^{18}O$ and δD. All of the isotope values are reported in parts per mil (‰) relative to the international standard, Vienna Standard Mean Ocean Water (VSMOW), in delta (δ) notation.

The $\delta^{18}O$ composition in the modern aragonite precipitation scraped from the glass plates (hereafter referred to as "$\delta^{18}O_{aragonite}$") was measured using a MAT-253 mass spectrometer linked to a Gas Bench-II (Thermo Electron Corporation, Bremen, Germany) at the Stable Isotope Centre of Fujian Normal University, China. The accuracy and precision were routinely checked by running the carbonate standard, CAI-13, which was carefully calibrated using NBS-18 and NBS-19 after every six sample measurements. The precision was better than 0.1‰. All of the oxygen isotope values are reported in parts per mil (‰) relative to the VPDB in delta (δ) notation.

3.4 Data analysis

The Pearson correlation analysis was performed to identify the strength of relationships using the SPSS software program version 16 (SPSS, Chicago, USA). Scatter plots were used to test the linear relationship between parameters. Climate datasets, including precipitation and temperature, were derived from the MHS (AD 1911–2013: 19°18′N, 97°50′E; 268 m a.s.l.) and PMP (AD 1987–2013: 19°31′N, 98°15′E; 800 m a.s.l.) meteorological stations (Thailand Meteorological Department 2013) (Fig. 1 a and c–d). The stable isotope ratios in the precipitate from Bangkok (BKK) (AD 1968–2004: 13°44′N, 100°34′E; 3 m a.s.l.) and Yangon (YG) (AD 1961–1963: 16°46′N, 96°10′E; 20 m a.s.l.) from the Global Network of Isotopes in Precipitation (GNIP) stations (IAEA/WMO 2001) were also used for comparison purposes (Fig. 1 a and c–d).

The moisture sources were identified using deuterium excess (d-excess) and air mass backward trajectory analyses. The d-excess values have been widely used as an indicator of non-equilibrium and evaporation processes (Dansgaard 1964). Deuterium excess is a function of $\delta^{18}O$ and δD in water which was defined as (Eq. 1) (Dansgaard 1964):

$$\text{Deuterium excess} = \delta D - 8 \times \delta^{18}O \qquad (1)$$

Trajectory analyses are commonly used to trace the source regions of air masses and moisture transportation into a given area (Ryoo et al. 2011; Hondula et al. 2010). For simplicity, trajectory analyses were performed to generate air mass trajectories as an indicator of changes in moisture transport paths and vapor sources. The data were obtained from the NOAA Air Resources Laboratory, Silver Spring, MD, USA, using the HYSPLIT model available at https://ready.arl.noaa.gov/HYSPLIT.php (Stein et al. 2015). The 72-h back trajectories starting at 500, 1,000, and 1,500 m above ground level were produced for each rain seasons, including the early rainy month (June) and the late rainy month (October). The trajectories were calculated for the whole month between the 1st and 30th of June 2012 as well as between the 1st and 31th of October 2012 at the NJ cave.

4 Results

4.1 Local atmospheric climate variability

The CF station received an annual rainfall total of 1129.5 mm (Fig. 1c), which was a ~ 10% higher rainfall quantity than that of the NJV station (Fig. 1d). The monthly rainfall totals demonstrated a strong primary wet (rainy) season beginning from May and continuing into October, while the dry (winter and summer) season started from November and lasted until the next April (Fig. 1 c and d). The rainy season accounted for more than 80% of the total annual rainfall for both the CF and NJV stations. As previously observed at other meteorological stations (Fig. 1 c and d), heterogeneous patterns of rainfall were also clearly evident at our monitoring stations (Fig. 1 c and d). Since the rainfall maximum only occurs once a year (August–September), the rainfall pattern for the CF station can be characterized as having a monomodal rainfall distribution (Fig. 1c). This monomodal pattern is similar to those observed in the YG (IAEA/WMO 2001) and MHS (Thai Meteorological Department 2013) stations (Fig. 1c). On the contrary, the NJV, BKK (IAEA/WMO 2001), and PMP (Thai Meteorological Department 2013) stations have bimodal rainfall distributions, with the first rainfall maximum in the early rainy season (May and June) and the second rainfall maximum in the late rainy season (August and September) (Fig. 1d).

The monthly (Fig. 1c–d and Fig. 2a) and daily (Fig. 2b) average temperatures and RH revealed similar variations at all stations. At the NJV station, during the cold months in winter (November to the following February), the monthly (Fig. 1c–d) and daily (Fig. 2b) average temperatures dropped to 17 °C (Fig. 1d). In the summer months, the temperatures greatly increased in April, with temperature maximums of 30.6 °C (Fig. 1d). The monthly average RH dropped to as low as 42–43% in the hot summer weather (Fig. 1d). However, both the temperatures and RH values were stable during the wet period of the rainy season (Fig. 2 a and b).

In general, the overall climate variability during the monitoring time period at both the NJV and CF stations is comparable to the long-term averaged patterns based on the dataset of local meteorological stations (MHS and PMP stations) (Thai Meteorological Department 2013), as well as the GNIP stations at Bangkok and Yangon (IAEA/WMO 2001) (Fig. 1 a and c–d and Fig. 2a). In addition, our monitoring results further confirmed the strong seasonality of the atmospheric climate variability in this region.

4.2 Cave microclimate conditions

The microclimate conditions within the NJ cave were significantly influenced by the atmospheric climate to varying degrees at different drip sites. The microclimate conditions

followed the atmospheric changes but exhibited smaller amplitudes in their variations (Fig. 2 a and b). The monthly and daily average values of the cave's temperatures and RH showed very close relationships with the external climate measured at the NJV station at the first sampling site near the cave entrance (CH-1) (daily temperature $r = 0.86$, $p < 0.01$, $n = 374$; daily RH $r = 0.87$, $p < 0.01$, $n = 374$), as well as in the interior of the cave (CH-2) (daily temperature $r = 0.57$, $p < 0.01$, $n = 311$; daily RH $r = 0.90$, $p < 0.01$, $n = 311$) (Fig. 2 a and b). At the CH-1, the monthly average temperatures and RH values were 23.1 °C and 72.7%, respectively (Fig. 2 a and b). However, the temperatures recorded at CH-2 remained more constant (varied from 21.5 to 22.2 °C) than those at CH-1, with a smaller amplitude of temperature change than that of the external temperatures and at CH-1, approximately 14 °C and 4 °C, respectively (Fig. 2 a and b). The cave microclimate showed a strong seasonality in response to the surface climate for both the wet and dry seasons (Fig. 2 a and b), except for the temperature variations at CH-2 (Fig. 2 a and b). Based on the available CO_2 data on May 5, 2018, the averaged concentrations of cave air CO_2 were approximately 750 ppm and 900 ppm at CH-1 and CH-2, respectively. Climate conditions outside the cave apparently control microclimate conditions inside the cave, especially the locations near the cave entrance (CH-1). However, at deep location inside the cave (CH-2) where this monitoring site was located at the end of the main chamber with the close environment conditions, it was less controlled by the outside thermal gradient due to the less air exchange.

4.3 Stable isotopic compositions in precipitation

Generally, the time series of rainfall $\delta^{18}O$ values at the NJV and CF stations are remarkably similar, even though they are different in the monthly distributions of the rainfall amount. The isotopic compositions of rainfall in the dry season (winter and summer months) were more enriched relative to those of the wet season (Fig. 1 c and d).

For the rainy season, the amount-weighted rainfall $\delta^{18}O$ values (hereafter referred to as "$\delta^{18}O_{Rain}$") during the early rainy months varied from − 1.3 to − 6.6‰ at the CF station and from − 1.2 to − 7.3‰ at the NJV station (Fig. 1 c and d), whereas the $\delta^{18}O_{Rain}$ values during the late rainy months fell within the range between − 5.9 and − 10.6‰ at the CF station and between − 4.6 and − 11.1‰ at the NJV station (Fig. 1 c and d). However, there was no observed relationship between rainfall $\delta^{18}O$ and its amount for both the CF and NJV stations (data not shown) during the rainy season.

Although a heterogeneous distribution of rainfall was clearly observed during the whole rainy season, the isotopic compositions of rainfall at the four stations (BKK, YG, CF, and NJV) exhibited a consistent intraseasonal pattern that was more enriched in $\delta^{18}O_{Rain}$ values during the early rainy season
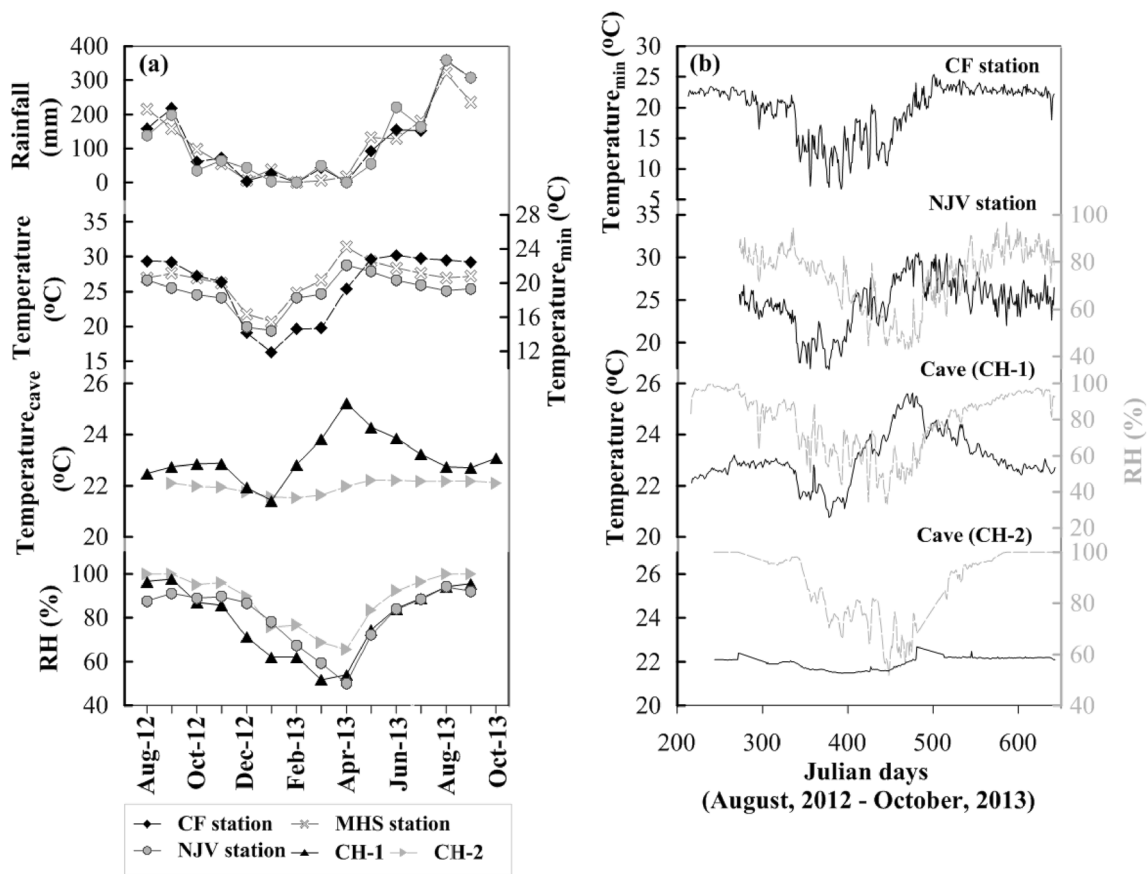
Fig. 2 Monthly (**a**) and daily (**b**) temporal variations in rainfall amount, surface temperature, cave air temperature (Temperature$_{cave}$), and relative humidity (RH) at NJV, CF, and MHS stations and the NJ cave (CH-1 and CH-2), except for the temperature at the CF station, which was measured as minimum temperature (temperature$_{min}$)

(Fig. 1 c and d). During the late rainy season, a clear decreasing shift in the monthly average $\delta^{18}O_{Rain}$ was observed, ~ 3.2‰ at the CF station and ~ 2.6‰ at the NJV station, which were lower values than those of the early rainy season (Fig. 1 c and d). This trend matched the long-term averaged seasonal pattern of $\delta^{18}O_{Rain}$ at the BKK and YG stations (Fig. 1 c and d), which had higher $\delta^{18}O_{Rain}$ values in the early rainy season and lower values in the late rainy season (Fig. 1 c and d), demonstrating that intra-rainy season patterns of $\delta^{18}O_{Rain}$ are a large regional rather than a local feature.

4.4 Stable isotopic compositions in cave drip waters

Overall, the values of $\delta^{18}O$ in cave drip water (hereafter referred to as "$\delta^{18}O_{DW}$") ranged from − 6.80 to − 2.46‰ (a mean value of − 5.1‰) at NJ-1, from − 6.74 to − 3.55‰ (a mean value of − 5.61‰) at NJ-1202, and from − 7.03 to − 1.56‰ (a mean value of − 5.16‰) at NJ-1203 drip sampling sites. The seasonal variations in $\delta^{18}O_{DW}$ (Fig. 3 a and b) closely resembled the variation observed in $\delta^{18}O_{Rain}$ at the NJV station (Fig. 3 a and b). The more enriched in $\delta^{18}O_{DW}$ values were generally observed at the early rainy season and gradually depleted towards the late rainy season (Fig. 3 a and

b). However, the mean value in rainfall $\delta^{18}O$ (− 6.92‰) was more negative than the $\delta^{18}O_{DW}$ values (~ 1.6, 1.5, and 1.8‰ for NJ-1, NJ-1202, and NJ-1203, respectively), indicating that the typical seasonal and intraseasonal variations in $\delta^{18}O_{Rain}$ were preserved in the $\delta^{18}O_{DW}$ signals, but their absolute values were modified in epikarst and/or in cave processions. The monthly mean $\delta^{18}O_{DW}$ values for all drip sites were smaller in the rainy season and higher in the dry seasons and shifted from approximately − 4 in the early rainy months to approximately − 6‰ in the late rainy months (Fig. 3b). Most of the accumulated drip water samples, except those in September, were more enriched in $\delta^{18}O_{DW}$ values than those in instantaneous drip water samples (Fig. 4c).

4.5 Drip water characteristics

All three drip sites were hydrologically active from a summer season in April to a winter season in December. The drip rate of NJ-1 ranged from 0.23 drips/minute to 1.06 drips/minute, with a mean value of 0.49 drips/minute, whereas the drip rate of NJ-1202 had a mean value of 0.28 drips/minute, with a maximum value of 0.43 drips/minute. The drip rate of NJ-1203 changed between 0.11 drips/minute and 0.24 drips/
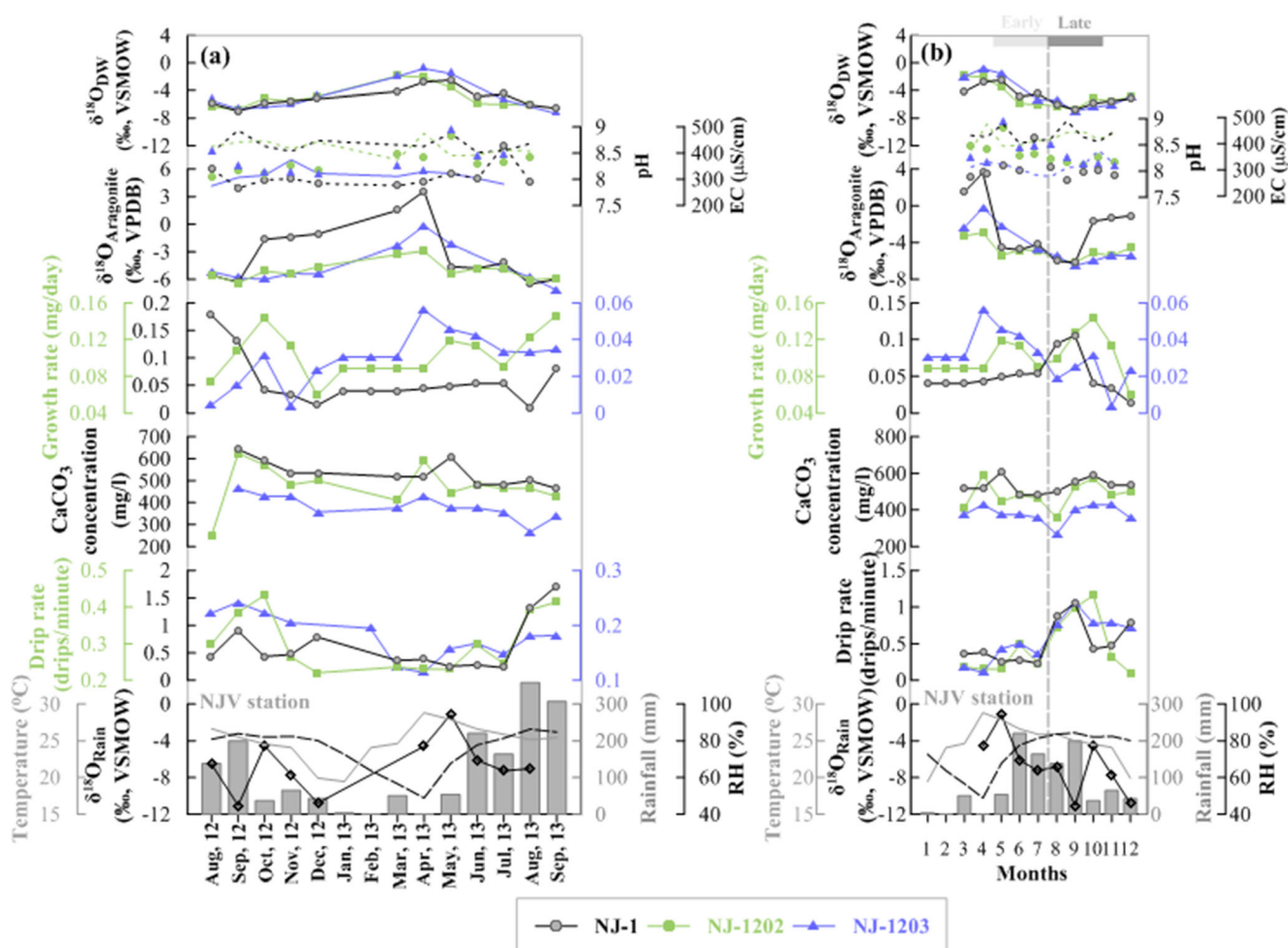
Fig. 3 a Temporal variations and b monthly average values of climate parameters outside the cave at the NJV station including rainfall amount (gray vertical bars); surface temperature (gray solid line); relative humidity (RH) (black dashed line); rainfall $\delta^{18}O$ ($\delta^{18}O_{Rain}$) (black solid line with open diamond); and stalagmite monitoring parameters including the $\delta^{18}O$ values of drip water ($\delta^{18}O_{DW}$), modern aragonite precipitated on glass places ($\delta^{18}O_{aragonite}$), stalagmite growth rate, drip rate, and drip water $CaCO_3$ concentration at NJ-1 (black line with filled gray circles),

NJ-1202 (green line with filled circles), and NJ-1203 (blue line with filled triangle symbols) drip sampling sites as well as the pH and EC values, respectively at NJ-1 (gray circle symbols and gray dashed line, respectively), NJ-1202 (green circle symbols and green dashed line, respectively), and NJ-1203 (blue triangle symbols and blue dashed line, respectively) drip sampling sites. The vertical dashed line in b indicates the boundary between early and late rainy seasons

minute, with a mean value of 0.17 drips/minute (Fig. 3 a and b). The drip rates generally decreased from early winter (~ March) to the early rainy months (MJJ) (0.26, 0.26, and 0.16 drips/minute for NJ-1, NJ-1202, and NJ-1203, respectively) and gradually increased until reaching the maximum rate in September (1.06 and 0.24 drips/minute for NJ-1 and NJ-1203, respectively) and October (0.43 drips/minute for NJ-1202) during the late rainy months (Fig. 3 a and b). There were no clear seasonal patterns observed for pH and EC, but they are likely to be bimodal cycles for $CaCO_3$ concentration. Variations of pH values varied between 7.8 and 8.6 for the NJ-1, 8.1 and 8.8 for the NJ-1202, and 8.1 and 9.0 for NJ-1203 (Fig. 3 a and b). The highest pH values were generally observed in May (NJ-1202 and NJ-1203) and July (NJ-1) (Fig. 3 a and b). However, the EC values of cave drip water vary and are likely inconsistent among sampling sites (Fig. 3 a

and b). The EC values ranged from 403 to 486 μS/cm for the NJ-1, from 390 to 446 μS/cm for the NJ-1202, and from 274 to 321 μS/cm for the NJ-1203. There were 2 months of the highest EC values occurring in May and September for the NJ-1 drip site. This was similar to the variation seen in the $CaCO_3$ concentration of the NJ-1(Fig. 3 a and b). The other sampling sites exhibited a dominant peak of EC in April (NJ-1202) and November (NJ-1203) (Fig. 3 a and b). The average values of the $CaCO_3$ concentration were 536, 475, and 367 mg/l at drip sites NJ-1, NJ-1202, and NJ-1203, respectively. The $CaCO_3$ concentration were most likely to be bimodal cycles (Fig. 3 a and b), with the first peak occurring in either April (NJ-1202 and NJ-1203) or May (NJ-1) and the secondary peak occurring in October (Fig. 3b). The lowest concentration was found in June at the NJ-1 drip site and in August at the rest of the drip sampling sites (Fig. 3 a and b).
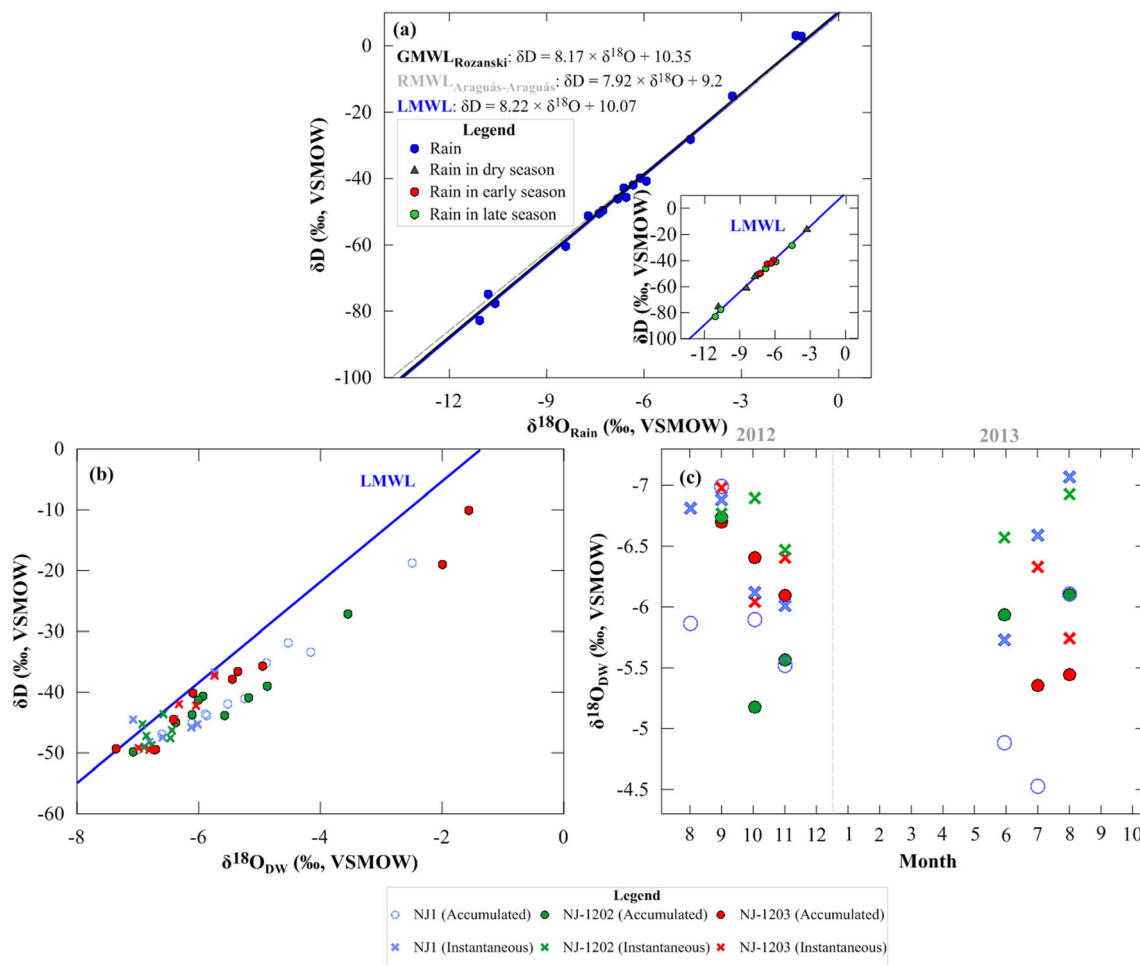
Fig. 4 Correlational analyses between δD and $\delta^{18}O$ in a the precipitation for the GMWL (black solid line) (Rozanski et al. 1993), the RMWL (gray dashed line) (Araguás-Araguás et al. 1998), and the LMWL (blue solid line) in present study. The inserted figure shows the plot of δD and $\delta^{18}O$ along the LMWL for different seasons. b Accumulated drip waters (circle symbols) and instantaneous drip waters (asterisk symbols) plotting below the LMWL. c Comparison between $\delta^{18}O_{DW}$ values of accumulated and instantaneous drip water samples

4.6 Growth rates of modern speleothem deposits

The extreme maximums in the NJ-1 growth rate were found only during the late rainy months in August and September (Fig. 3 a and b). The deposition rate at NJ-1202 (a mean value of 0.11 g/month) exhibited higher values in its deposition rate than those of NJ-1 (a mean value of 0.07 g/month) and NJ-1203 (a mean value of 0.04 g/month) (Fig. 3 a and b).

4.7 Oxygen isotopic composition in modern speleothem deposits

$\delta^{18}O_{aragonite}$ precipitated on glass plate substrates ranged from − 6.5 to 3.6‰, − 6.4 to − 2.9‰, and − 7.2 to − 0.2‰, with mean values of − 3.08‰, − 5.02‰, and − 4.56‰ for NJ-1, NJ-1202, and NJ-1203, respectively. The variations in $\delta^{18}O_{aragonite}$ showed obvious seasonal and intraseasonal variations, which were similar to those of their feeding drip water, with more positive values during the dry (winter and summer)

season and in the early rainy season, whereas more negative values were obtained in the late rainy season (Fig. 3 a and b).

5 Discussion

5.1 on the isotopic compositions of precipitation

5.1.1 Local meteoric water line

As there are relatively few rainfall isotopic data in Thailand, the first local meteoric water line (LMWL) of NW Thailand was constructed and plotted against the reference meteoric water lines, including (1) the global meteoric water line (GMWL) (Rozanski et al. 1993) and (2) the regional meteoric water lines (RMWL) of Southeast Asia (Araguás-Araguás et al. 1998). This study is the preliminary due to the sparse datasets. The LMWL ($r^2 = 0.991$, $n = 16$) (Eq. 2) was defined using monthly rainfall samples from the NJV and CF stations

over the monitoring period as:

$$LMWL: \delta D = 8.22 \times \delta^{18}O + 10.07 \qquad (2)$$

The plots of the $\delta^{18}O_{Rain}$ values were generally clustered along the GMWL and RMWL (Fig. 4a) and showed little deviation from these reference lines during the dry season and late rainy season (Fig. 4a). These results indicated that the isotopic composition of precipitation in the study site reflected the isotopic composition of the regional meteoric precipitation.

5.1.2 Effects of changes in moisture sources

Among the other effects influencing oxygen isotopes in meteoric water, the rainfall amount is one of the dominant contributors to $\delta^{18}O_{Rain}$ in the tropical and subtropical regions, with an inverse relationship between rainfall $\delta^{18}O$ and its amount (Rozanski et al. 1993; Araguás-Araguás et al. 1998). We evaluated this relationship and found that there was no observed correlation between the two variables at the monthly time scale. Previous studies have reported that isotopic variations in present-day Asian monsoon precipitation, especially in the Southeast Asian region, are controlled by moisture source regimes rather than local precipitation amounts and temperature (Aggarwal et al. 2004; Sengupta and Sarkar 2006; Le Duy et al. 2018; Wei et al. 2018). Moisture transported from the Indian Ocean is characterized by less negative $\delta^{18}O$ values, while the air circulation regime induces a higher flux of isotopically depleted moisture that is transported from the western tropical Pacific Ocean, resulting in more negative $\delta^{18}O$ values (Aggarwal et al. 2004). d-excess in precipitation has been used as a useful tracer of the origin of atmospheric vapor (Rozanski et al. 1993). The moisture source originating from the Indian Ocean is often associated with higher d-excess values (> 10‰) compared with that from the Pacific Ocean (Fröhlich et al. 2002; Bershaw 2018) due to the lower d-excess values of summer precipitation originated from the Pacific Ocean (Bershaw 2018). The d-excess values of rain water also exhibited intraseasonal variations (Fig. 5). The d-excess values in the early rainy season were quite high and were centered on a narrow range (Fig. 5). By comparison, the d-excess values in the late rainy season were spread over a larger range, with lower values during the major rainfall peak in September (Fig. 5).

Although secondary evaporation in the process of falling raindrops can also result in lower d-excess values, the higher RH and lower temperature during the late rainy season, especially in September, indicated that secondary evaporation could not be the reason for this intraseasonal diversity in d-excess. The lower d-excess values in September indicated that moisture mainly came from the Pacific Ocean. Hence, the intraseasonal feature of d-excess indicated that the moisture
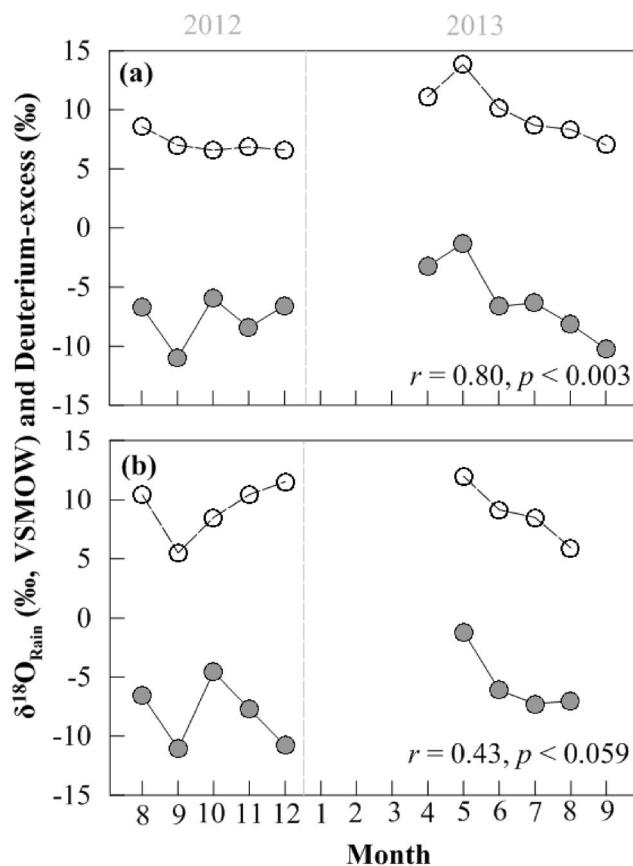
Fig. 5 Monthly temporal variations of $\delta^{18}O_{Rain}$ (solid circles) and deuterium excess values (open circles) for a CF and b NJV stations. Note that the seasonal $\delta^{18}O_{Rain}$ and deuterium excess data during the dry season were excluded

that contributes to this area during the early rainy season shows unicity and points to the Indian Ocean, while the moisture source for the late rainy season is much more complex, with its important contributor likely being the west Pacific Ocean.

Air trajectory models were used to demonstrate the source of the air parcels that produce precipitation at a specific location (Ryoo et al. 2011; Hondula et al. 2010). Preliminary analyses of the air mass trajectories in the study site confirmed that the moisture contributed from the tropical Indian Ocean generated the early season rain (Fig. 6a) and revealed more enriched $\delta^{18}O$ values (Fig. 3 a and b), whereas most of the moisture during the late season rain, which had more depleted $\delta^{18}O$ values (Fig. 3 a and b), was a mixing of air masses originating from the Indian Ocean as well as the continental air mass from mainland China, maritime air masses from the South China Sea (SCS), and western North Pacific (WNP) Ocean (Fig. 6b). The results implied that $\delta^{18}O_{Rain}$ in our study site was more related to moisture sources and transport patterns rather than to the local amount effect. Variations in TM $\delta^{18}O_{Rain}$ values result from the sources
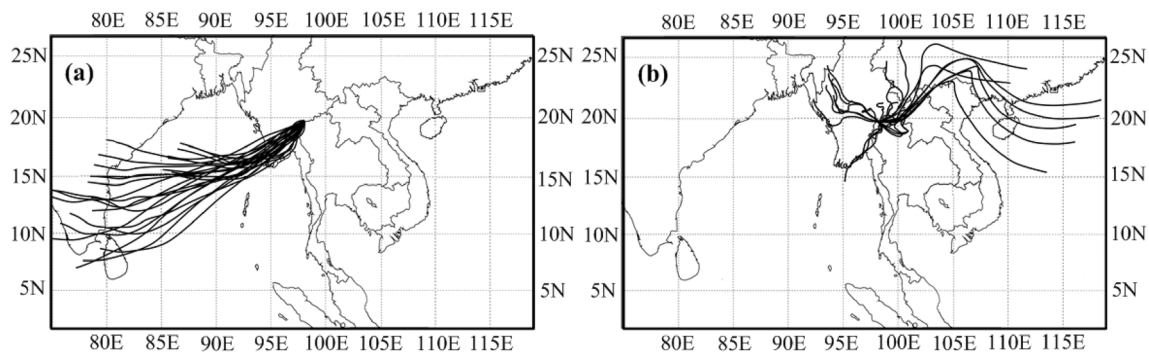
Fig. 6 The 72-h back trajectories starting at 500, 1,000, and 1,500 m above ground level (Stein et al. 2015) for **a** early rainy month (June) and **b** late rainy month (October) at the NJ cave location

of moisture where an air mass originates. There is strong evidence supporting the potential use of stalagmite stable isotopes to detect dual vapor sources and transport pathways.

5.2 Controls of speleothem oxygen isotopes ($\delta^{18}O$)

5.2.1 Factors controlling $\delta^{18}O$ in drip water

For perennial drip in caves with a thick overlying bedrock, the $\delta^{18}O_{DW}$ values are thought to be (or close to) representative of the mean value of yearly or multi-yearly rainfall (e.g., Duan et al. 2016; Wang et al. 2016). In general, $\delta^{18}O_{DW}$ follows the variations in $\delta^{18}O_{Rain}$ and exhibits a similar seasonal mode, indicating the rapid response of $\delta^{18}O_{DW}$ to $\delta^{18}O_{Rain}$ and that $\delta^{18}O_{DW}$ inherits the seasonal pattern of $\delta^{18}O_{Rain}$. However, it should be noted that this seasonal trend is superimposed with other processes. Compared with the weighted $\delta^{18}O_{Rain}$ values, the $\delta^{18}O_{DW}$ values are enriched to different extents, with different scopes of discrepancy among the three monitoring drip sites (Figs. 3 and 4). The only exception occurs in September. In September, the $\delta^{18}O_{DW}$ values for all drip sites are roughly similar and are nearly close to the weighted $\delta^{18}O_{Rain}$. In the diagram of δD-$\delta^{18}O$, the drip water isotopic values are shown to be below the LMWL (Fig. 4b), suggesting that secondary evaporation should occur in the infiltration processes through the epikarst and (or) discharge processes in the cave. Taking the drip rate curves into consideration, it seems that evaporation most likely occurs in the cave process. The drip rates for all of the drip sites show a similar response pattern. Although their absolute values are quite different, they abruptly increase in September and then slowly decrease (Fig. 3). The drip rate and relative humidity maximums (Fig. 3) coincide with the isotopic homogenization among all drip sites, with more negative $\delta^{18}O_{DW}$ values in September, demonstrating that isotopic homogenization among different drip sites in other months should occur in the cave (Fig. 3 a and b). The heterogenization of $\delta^{18}O_{DW}$ among the drip sites arose from the different discharge rates and different cave micro-environments of each drip site, e.g., the ceiling height and location of the drip site,

when both the RH of the cave and drip rate are low. The comparison between the $\delta^{18}O_{DW}$ values in accumulated drip water and those of collected instantaneously gives additional evidence for the evaporation effect in the cave. The evaporation effect is strong during the dry season and is relatively weaker during the early rainy season (Fig. 4c).

In short, the variations in the $\delta^{18}O_{DW}$ values in the NJ cave followed the changes in the $\delta^{18}O_{Rain}$ values, exhibiting a discernible seasonal pattern with much heavier values in the dry and early rainy seasons than those in the late rainy season, especially in September (might also be in the late August). The $\delta^{18}O_{DW}$ values in the late rainy season were close to the weighted average value of $\delta^{18}O_{Rain}$ and exhibited homogeneity among the drip sites, while the values in the dry season were more enriched in $\delta^{18}O_{DW}$ due to the evaporation effect in the cave, resulting in heterogeneous values among the drip sites. The $\delta^{18}O_{DW}$ values in the early rainy season were influenced by a heavier $\delta^{18}O_{Rain}$ input and were superimposed by small effect of evaporation, resulting in higher values than those in the late rainy season.

5.2.2 Oxygen isotopic fractionation between modern aragonite precipitation on glass plate and drip water

Evaluating the dominant controlling factors of speleothem $\delta^{18}O$ and the fractionation behavior appears to be necessary to correctly interpret the isotopic signals as well as to select suitable speleothem samples for extracting paleoclimate data (Li et al. 2011; Pu et al. 2016). The two equations of Patterson et al. (1993) and Kim et al. (2007) were applied to calculate the aragonite-water fractionation equations and the expected speleothem $\delta^{18}O$ deposits at equilibrium conditions (Tables 1 and 2). The measured $\delta^{18}O_{aragonite}$ values of modern aragonite precipitated on glass plates were more equivalent to the expected $\delta^{18}O_{aragonite}$ values calculated from the equation of Kim et al. (2007) than those of Patterson et al. (1993), with only slightly different values of 0.09‰ for NJ-1202 and 0.01‰ for NJ-1203 (Table 1). These results implied that the stalagmites under the NJ-1202 and NJ-1203 drip sampling sites were deposited at or close to isotopic equilibrium

Oxygen isotopic compositions of meteoric precipitation, drip water, and aragonitic stalagmite deposition...

739

Table 1 Measured and calculated average $\delta^{18}O$ values of modern speleothem deposits from the Namjang cave for the interval of approximately AD 2012 to 2013

Samples	Measured $\delta^{18}O_{aragonite}$ (‰, VPDB)	Measured[a] $\delta^{18}O_{DW}$ (‰, VSMOW)	Temp.$_{DW}$ (°C)	Equation from Patterson et al. (1993)[b]			Equation from Kim et al. (2007)[c]		
				$\alpha_{aragonite-water}$	$1000ln\alpha_{aragonite-water}$	Predicted $\delta^{18}O_{aragonite}$ (‰, VPDB)	$\alpha_{aragonite-water}$	$1000ln\alpha_{aragonite-water}$	Predicted $\delta^{18}O_{aragonite}$ (‰, VPDB)
NJ-1	− 3.08	− 5.09	22.84	1.03063	30.17	− 5.37	1.03108	30.61	− 4.93
NJ-1$_{Rain}$	− 5.13	− 5.60	23.09	1.03057	30.12	− 5.93	1.03102	30.55	− 5.49
NJ-1202	− 5.02	− 5.11	22.71	1.03065	30.19	− 5.37	1.03111	30.63	− 4.93
NJ-1203	− 4.56	− 4.86	22.20	1.03076	30.00	− 5.01	1.03122	30.74	− 4.57

[a] The VSMOW to the VPDB conversions of drip water $\delta^{18}O$ values ($\delta^{18}O_{DW}$) was calculated from the expression of Coplen et al. (2002): $\delta^{18}O_{VPDB} = 0.97001\delta^{18}O_{VSMOW} − 29.99$

[b] Aragonite–water fractionation equation by Patterson et al. (1993): $100ln\alpha_{aragonite-water} = 18.56 \pm 0.32 (10^3/T) − 33.49 \pm 0.31$ [c] Aragonite–water fractionation equation by Kim et al. (2007): $100ln\alpha_{aragonite-water} = 17.88 \pm 0.13 (10^3/T) − 31.14 \pm 0.46$

conditions. At the NJ-1 drip sampling site, the $\delta^{18}O_{aragonite}$ values were almost 0.5–2‰ dry months, which probably represent higher than the values calculated by Patterson et al. (1993) and Kim et al. (2007) (Table 1). This result indicated the presence of significant kinetic fractionation during the aragonite precipitation of the stalagmite formed under the NJ-1 drip sampling site. The possible mechanisms relating the disequilibrium isotopic fractionations include the evaporation driving the supersaturation of drip water, leading to an isotope-enriched drip water solution and the rapid degassing of CO_2 from water during stalagmite deposition (Hendy 1971). Previous study showed that the growing rate and $\delta^{18}O$ values of stalagmite NJ-1 depend largely on the portions

of early and late rains. Thus, the stalagmite deposited under the NI-1 drip site is most influenced by rainfall during the rainy season and is less influenced by a less (or no) rain during the dry season (Cai et al. 2010). Typically, the disequilibrium conditions occur when the cave RH is low. According to the monitoring data in this study, the atmosphere of the NJ cave becomes progressively drier during the summer and winter months, with an average RH value of 58%, and wetter during rainy months, with an average RH value of 95% for the cave interior. This evaporation process should have slight but negligible influences on the stalagmite NJ-1 deposits during the rainy season when the cave RH remains close to 100%. The aragonite-water fractionations at the NJ-1 drip sampling site

Table 2 Measured and calculated monthly $\delta^{18}O$ values of modern deposits under the drip water which feed the stalagmite NJ-1 for the interval of approximately AD 2012 to 2013

Month/ year	Measured $\delta^{18}O_{aragonite}$ (‰, VPDB)	Measured[a] $\delta^{18}O_{DW}$ (‰, VSMOW)	Temp.$_{DW}$ (°C)	Equation from Patterson et al. (1993)[b]			Equation from Kim et al. (2007)[c]		
				$\alpha_{aragonite-water}$	$1000ln\alpha_{aragonite-water}$	Predicted $\delta^{18}O_{aragonite}$ (‰, VPDB)	$\alpha_{aragonite-water}$	$1000ln\alpha_{aragonite-water}$	Predicted $\delta^{18}O_{aragonite}$ (‰, VPDB)
08/2012	− 5.57	− 5.86	22.75	1.03064	30.18448	− 6.13	1.03110	30.62463	− 5.69
09/2012	− 6.31	− 7.00	22.71	1.03065	30.19258	− 7.25	1.03111	30.63312	− 6.81
10/2012	− 1.68	− 5.90	22.86	1.03062	30.16313	− 6.18	1.03107	30.60225	− 5.75
11/2012	− 1.37	− 5.52	22.89	1.03062	30.15721	− 5.81	1.03107	30.59604	− 5.37
12/2012	− 1.08	− 5.24	21.93	1.03082	30.35338	− 5.33	1.03128	30.80169	− 4.89
03/2013	1.51	− 4.16	23.83	1.03042	2996414	− 4.65	1.03086	30.39365	− 4.22
05/2013	− 2.49	− 4.60	24.30	1.02847	28.07481	− 4.86	1.02854	28.14217	− 4.79
06/2013	− 4.79	− 4.88	23.86	1.03041	29.95830	− 5.37	1.03085	30.38753	− 4.95
07/2013	− 4.20	− 4.53	23.24	1.03054	30.08491	− 4.89	1.03099	30.52025	− 4.46
08/2013	− 6.50	− 6.12	22.48	1.03070	30.2399	− 6.32	1.03052	30.06273	− 6.49
09/2013	− 5.99	− 7.00	22.75	1.03064	30.18477	− 7.26	1.03110	30.62493	− 6.82
10/2013	− 6.50	− 7.00	22.86	1.03062	30.16313	− 6.88	1.03107	30.60225	− 6.45

[a, b, c] Dataset was calculated as in Table 1

were further calculated with separate month values with the assumption that the disequilibrium condition could only occur in dry months (i.e., from November 2012 to April 2013) when the cave air RH was very low (Table 2). Most of the $\delta^{18}O_{aragonite}$ values measured during the rainy months were close to the theoretical value predicted by Kim et al. (2007) (Table 2). Comparisons between the measured and predicted modern $\delta^{18}O_{aragonite}$ values while excluding data from the dry months probably represent non-equilibrium conditions (NJ-1_{Rain}), indicating that the stalagmite that form under the NJ-1 drip sampling site was precipitated at or near oxygen isotopic equilibrium during the rainy season (Table 1). The average monthly $\delta^{18}O_{aragonite}$ values of the precipitate on glass plates ($-5.02‰$ and $-3.08‰$) were close to the published isotope data for the top of the fossil stalagmite NJ-1 ($-6.8‰$ and $-3.3‰$) (Cai et al. 2010). Although rapid water (i.e., rain and drip waters) flow rate associated with high CO_2 degassing rate of drip water can possibly lead to disequilibrium deposition for stalagmite NJ-1 during the rainy season, we were unable to determine this effect due to the lack of CO_2 equipment during the study period in AD 2012–2013.

For the drip site NJ-1202, it should be noted that the equilibrium condition during the dry season may be a presentational result in our monitoring experiment. The effect of evaporation on isotopic equilibrium should theoretically be similar for the NJ-1 and NJ-1202 drip sampling sites because both sites have similar RH with the low levels of RH during the dry season. However, the discrepancy between these two drip sites could be reasonably explained by the duration of carbonate precipitation. The NJ-1 is a drip site with bigger buffer where drip water abruptly slows down after the rainy season and then keeps stable with slow drip rate through the following dry season (Fig. 8). Therefore, the carbonate deposition occurred continuously during dry season that resulted in significant effects of evaporation. For the NJ-1202 drip site, the drips may stop periodically because of its small buffer. The time for the deposition of the NJ-1202 is much shorter than monitoring intervals, possibly short terms after the rainy season and (or) before the next rainy season. This short duration of stalagmite precipitations means less evaporation compared with the NJ-1. Unfortunately, we were unable to identify this possible process due to less frequent monitoring.

Overall, the $\delta^{18}O_{DW}$ values were clearly shown to exert a dominant control on $\delta^{18}O_{aragonite}$ (Fig. 7b). Successive interpretation of the stalagmite $\delta^{18}O$ value mainly depends upon the understanding of how the isotopic composition of meteoric precipitation was modified in cave drip water and thus preserved in the stalagmite. In this study, the results indicated that the variations in $\delta^{18}O$ values of stalagmites formed under the drip sites NJ-1202 and NJ-1203 were primarily a function of the variation in cave drip water $\delta^{18}O$ value, which in turn, were linked to the variability of rainfall $\delta^{18}O$. However, the $\delta^{18}O$ values of stalagmite NI-1 that likely experience non-

equilibrium conditions during its deposition in the dry season should be used with caution for further research.

5.3 Controls on speleothem growth rate

The monthly contents of the aragonite deposition for the three drip sites exhibited two reversed seasonal variation modes (Fig. 3b). For the drip sites NJ-1 and NJ-1202, the aragonite deposition rate follows the change in the drip rate, with peak values during the late rainy season from August to October and low values in the dry season from December to following July. Although the monthly average aragonite deposition and drip rate for the drip site NJ-1 generally show the similar variation trends (Fig. 3b), this observed patterns in 2013 indicate the possible 1-month lag (from August to September) of aragonite deposition (Fig. 3a). There were significant correlation between the drip rate and amount of carbonate precipitation for both NJ-1 ($r = 0.54$, $p < 0.040$, $n = 12$) and NJ-1202 ($r = 0.76$, $p < 0.004$, $n = 12$) (Fig. 8b), although the absolute values of both the deposition amount and drip rate at drip site NJ-1203 showed peaks during the summer dry season and early rainy season from April to June and then slowly decreased, with a significant negative correlation ($r = -0.72$, $p < 0.008$, $n = 12$) (Fig. 8b).

There are numerous parameters, e.g., the drip rate, Ca^{2+} concentration, ceiling height, temperature, and RH and CO_2 contents in cave air, that may influence carbonate precipitation from drip water (approximately to stalagmite growth) (Genty et al. 2001; Cai et al. 2011; Baker et al. 2007; Duan et al. 2011). Carbonate precipitation presupposes that the "mother" water is supersaturated. For a drip site with a high degree of saturation, the amount of precipitation will be directly controlled by the carbonate flux, which is a function of the drip rate and cation concentration in the feeding drip water. NJ-1 and NJ-1202 are representative of this case. The slow drip rate can extend degassing time. Monitoring sites are in a relatively large chamber and close to cave entrance, indicating a rapid exchange of cave air with outside air. This together with less discharge in the cave may contribute to low levels of air CO_2 inside the cave. The low concentration of cave air CO_2 of less than 1,000 ppm with long degassing prefers supersaturation of drip water (Cai et al. 2011; Duan et al. 2011; Pu et al. 2016). Therefore, the drip rate becomes the first controlling factor for the amount of carbonate precipitation. NJ-1203 is representative of another case in which the degree of saturation may be an important limitation for carbonate precipitation, as it was for other studies found in the Asian monsoon regions (Cai et al. 2011; Duan et al. 2011; Pu et al. 2016). The degree of saturation of drip water was mainly determined by the drip rate and cave air CO_2 level. In the rainy season, the CO_2 level abruptly increased in a closed chamber due to a large amount of water discharging into the cave. Although the long-term variations in cave air CO_2 data were unavailable during the
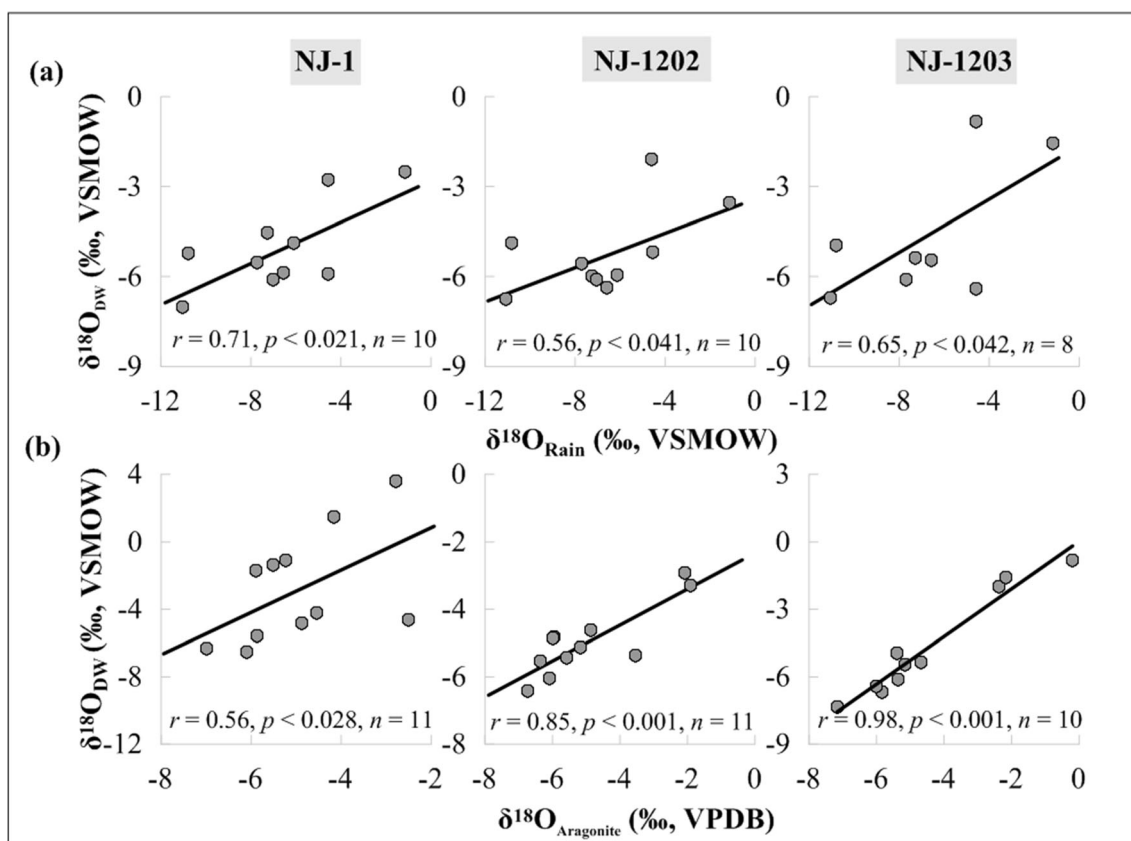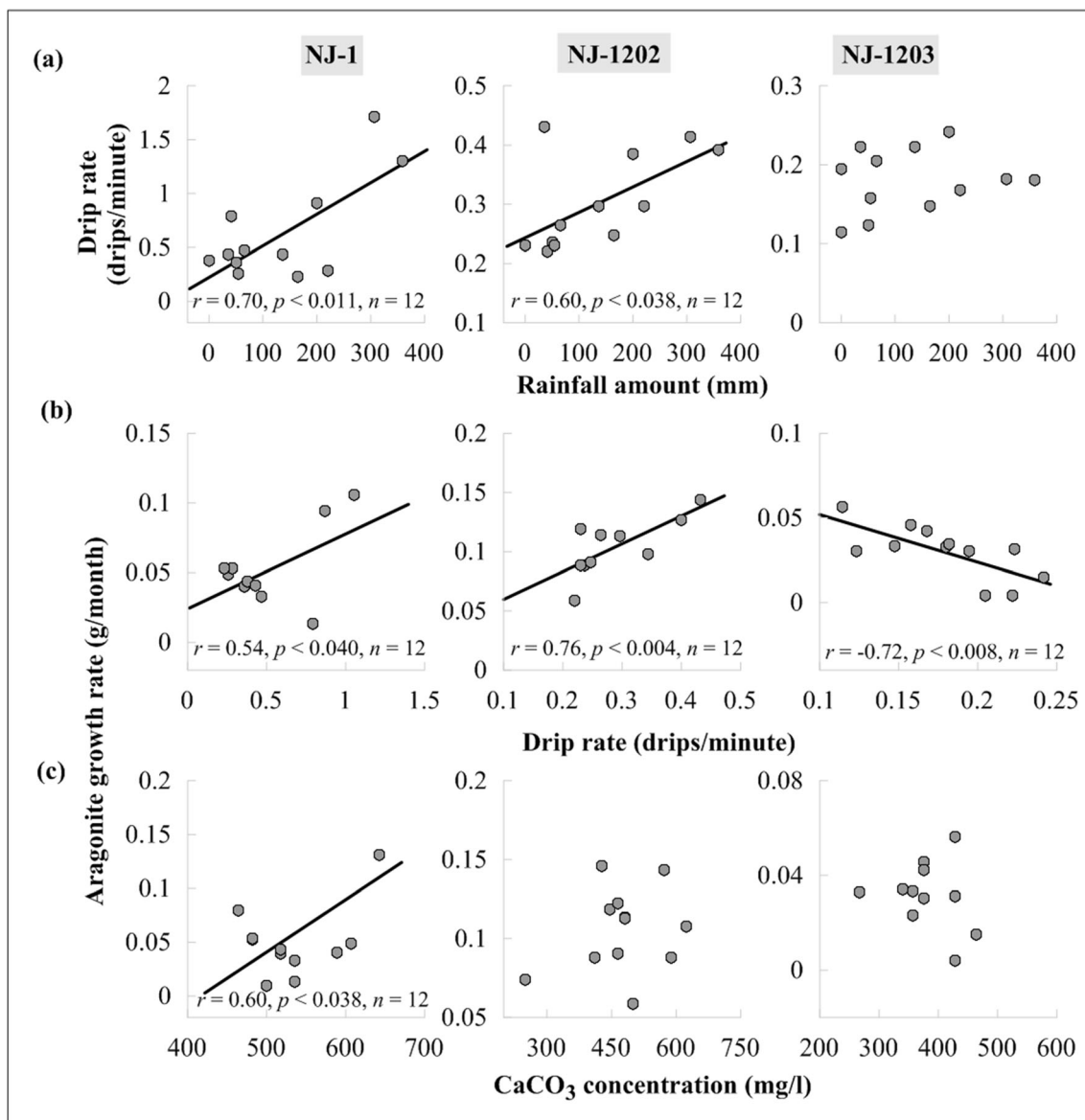
Fig. 7 Correlational analyses of drip water $\delta^{18}O$ ($\delta^{18}O_{DW}$) values with a rainfall $\delta^{18}O$ ($\delta^{18}O_{Rain}$) values and b modern aragonite $\delta^{18}O$ precipitates on glass plates ($\delta^{18}O_{aragonite}$) at NJ-1, NJ-1202, and NJ-1203 drip sampling site. Linear regressions are shown with black lines, r represents Pearson's correlation coefficient, and n is the number of data points

study period in AD 2012–2013, measurements of cave air CO_2 levels taken during cave visit in AD 2018 during the early rainy season showed that the cave air CO_2 concentrations in a close chamber (CH-2) was approximately 150 ppm higher than those in an open chamber (CH-1). Both the high discharge rate and high cave air CO_2 level reduced degassing and the degree of saturation in drip water, and thus reduced carbonate precipitation (Cai et al. 2011; Duan et al. 2011). Compared with the other two drip sites, the drip rate in NJ-1203 is similar to that in NJ-1202, both in the absolute value and seasonal pattern. The distinguishing difference in the environment between NJ-1203 and the other two drips is that NJ-1203 is located in the inner chamber, where the cave air CO_2 level may be much higher, which would reduce degassing and carbonate precipitation in the rainy season (Cai et al. 2011; Duan et al. 2011). Moreover, the lower $CaCO_3$ concentration associated with the higher drip rates observed in NJ-1203 is probably an additional factor affecting this negative correlation due to the smaller amount of calcium carbonate deposits forming a stalagmite. As a result, the amount of carbonate precipitation in NJ-1203 has a high negative correlation with the drip rate. The inverse response of carbonate precipitation to the drip rate in this cave indicates the complexity of the stalagmite growth rate, even in this

region. A successful interpretation of the stalagmite growth rate should be based on careful calibration. In this cave, the growth rate sequences derived from stalagmites from the outer chamber (saying NJ-1 and NJ-1202) can possibly be taken as an index of rainfall and are expected to be duplicated if their time scales are as promised.

The response of individual drips to the surface climate is strongly related to the characteristics of epikarst aquifers and the water flow in the unsaturated zone (Baker et al. 1997). The drip rates for all three drip sites do not increase obviously in the early rainy season. The drip rates reach their peak values until September, coinciding with the rainfall annual peak (Fig. 1 c and d), indicating that intense rainfall during the late rainy season contributes to more recharging water. An alternative explanation for this delayed response is that their buffer is large. However, much more transient drips in September were observed. Furthermore, NJ-1 rapidly responded to an intense rainfall in September 2012 (Fig. 3). This evidence implies that intense rainfall during the late rainy season likely contributes to more recharging underground water. A major rainfall peak during the late rainy season (August to October) contributes up to 51% of the summer monsoon rainfall in this region (Thai Meteorological Department 2013). The maximum in drip water flow rates in the late rainy season implied that higher ASO

Fig. 8 Correlational analyses of a drip rates versus rainfall amount at the NJV station, and stalagmite growth rates versus b drip rates and c drip water CaCO₃ concentration at NJ-1, NJ-1202, and NJ-1203 drip sampling sites. Linear regressions are shown as in Fig. 7

rainfall led to faster rates of the drip water feeding the stalagmites in NJ-1 and NJ-1202 (Fig. 3 a and b). Comparisons between the carbonate precipitation rates and drip rates at NJ-1 and NJ-1202 confirmed that the growing rates of the stalagmites under these drips are primary controlled by the drip water flow rates (Fig. 8b). Higher drip water flow rates with greater speleothem depositions at NJ-1 suggest a rapid response to surface rainfall and indicate a short residence time of rain waters stored in the unsaturated zone above the cave.

The growth rates of previously published stalagmites from the NJ cave are susceptible to seasonal climate forcing, particularly in the late rainy season (Cai et al. 2010; Muangsong et al. 2014). Our results further confirmed that the growing rates of the studied stalagmites from the NJ cave are primary controlled by the drip

water flow rates, which are linked to the amount of water recharge into the cave during the summer monsoon season. These results lead to an interpretation of the stalagmite growth rates derived from stalagmite NJ-1 and NJ-1202 being a reliable and robust proxy of the rainfall amount.

5.4 Implications for Thailand monsoon reconstruction

5.4.1 Implications for speleothem-based stable isotope record of TM

The seasonal pattern of $\delta^{18}O$ in local monsoon rainfall is closely related to that of a broad region in Southeast Asia, with relative less negative values in the early rainy season (May–June–July)

and lower values in the late rainy season (especially in September). Drip water $\delta^{18}O$ from the NJ cave could inherit the signals of rainfall $\delta^{18}O$ but is shaded by the evaporation effect in the cave and/or in the epikarst during the dry season and early rainy season. This effect overlaps the recharging rainfall signal, thus strengthening the seasonal change in $\delta^{18}O_{DW}$ and resulting in significant positive values in the dry season and early rainy season, with much negative values in the late rainy season. In some cases, this positive distortion could be further strengthened by non-equilibrium isotopic fraction that occurs in carbonate precipitation. For example, $\delta^{18}O$ in carbonate from drip site NJ-1 is a positive departure from feeding drip water during dry season. These monitored results demonstrate the complexity of the interpretation of the stalagmite $\delta^{18}O$ from this region, especially for a cave that undergoes seasonal changes in its environment. To better understand stalagmite $\delta^{18}O$, careful calibration with local meteorological data and data monitoring are necessary. For the NJ cave, the $\delta^{18}O$ records derived from different stalagmites may record different aspects of the climate history. Because the possible dynamic fraction effects act in the same direction as the seasonal pattern of rainfall, the stalagmite fed by drip at NJ-1 may record the seasonal impact of rainfall and emphasize the signal of rainfall in the late rainy season, especially in late August and September, because large carbonate deposition with a negligible dynamic fraction was influential during this time period (Fig. 3 a and b). A similar case should occur for the stalagmite fed by NJ-1202. However, the stalagmite fed by NJ-1203 may be of the other case due to the smaller carbonate deposition in the late rainy season. Therefore, the monitoring data used in this study further support our previous calibration result for stalagmite NJ-1, in which we found $\delta^{18}O$ in NJ-1 to have a strong negative relationship with rainfall in the late rainy season, especially in September, and we also found that it had a weak but significant positive relationship with rainfall during the early rainy season (MJJ) (Cai et al. 2010; Muangsong et al. 2011). The $\delta^{18}O$ values of stalagmite formed under drip sites NJ-1202 and NJ-1203 from the NJ cave can be regarded as a proxy of the seasonal variation in monsoon rainfall $\delta^{18}O$ and can be used to explore the history of moisture source trajectories in this region. Because isotope disequilibrium effects possibly affected stalagmite NJ-1 $\delta^{18}O$ values during the dry season, careful calibration and verification processes are required to further test the applicability of stalagmite NJ-1 $\delta^{18}O$ values.

5.4.2 Implications for speleothem-based growth rate record of TM

The seasonal variability in the amount of carbonate precipitation shows two inverse response patterns to the drip rate. For drip sites in a relatively open environment, e.g., drips NJ-1 and NJ-1202, moderate to strong positive relationships were found between the carbonate deposition amount and the feeding drip rate. The responses of individual drips to surface climate were strongly related to the rainfall amount. Increased amount of rainfall maintains drip water at a high level and increases the amount of the speleothem deposition. The extreme maximum growth rates at the NJ-1 drip site were amounts found during the late rainy months in August and September and were likely constant for the other months (Fig. 3 a and b), indicating that the NJ-1 growth rates were dominated by rainfall and drip water during the late rainy season. As a result, the NJ-1 growth rates could be best interpreted as a proxy for the amount of rainfall in the late rainy season or ASO rainfall. This result is accordant with the annual layer change in stalagmite NJ-1 (Cai et al. 2010). Although the NJ-1202 drip rates were induced by a high amount of late season rain, there were two periods with the highest growth rate at this drip site in both the early and late rainy seasons (Fig. 3 a and b). The growth rates of the stalagmite under the NJ-1202 drip site could have the greatest potential for high-resolution reconstructions of either ASO rainfall or the rainfall total during the whole summer monsoon season. The reverse is true of the drip sites NJ-1 and NJ-1202, and the seasonal variation in the amount of carbonate precipitation of the drip NJ-1203 is anti-correlated to the other drip sites due to less deposition in rainy season, while more deposition occurs in the succedent dry season. The additional rainfall in the rainy season, especially in the late rainy season, can maintain more flux in the following dry season. The annual deposition rate is also dependent on the rainfall amount, implying that $\delta^{18}O$ in the stalagmite fed by drip at NJ-1203 may be inappropriate for use in a paleoclimate study because most of the carbonate deposition occurred in the dry season and might be deeply influenced by dynamic effects. However, its growth rate could provide the rainfall history and is possibly comparable to other stalagmites, e.g., NJ-1 and NJ-1202, if their time scales can be well constructed.

5.4.3 Potential for developing multi-proxy climate reconstructions

Climatic information derived from multiple-proxy series generally improve the robustness of paleoclimate reconstructions (Smith et al. 2006; Li et al. 2010). The integration of proxy data from this area is a major challenge, as there are limited numbers of highly qualified climate proxies with an equivalent quality. Proxy indicators of Thailand's climate, including teak tree rings and stalagmites, are sensitive to seasonal climate forcing (Cai et al. 2010; Muangsong et al. 2016, 2018). Correlations of stalagmite $\delta^{18}O$ with the growth rate parameter (NJ-1 $r = -0.43$, $p < 0.030$, $n = 12$; NJ-1203 $r = 0.63$, $p < 0.025$, $n = 12$) and the factor controlling the growth rate (i.e., drip rate) (NJ-1 $r = -0.64$, $p < 0.025$, $n = 12$; NJ-1202 $r = -0.52$, $p < 0.036$, $n = 12$; NJ-1203 $r = -0.79$, $p < 0.11$, $n = 12$) strongly confirmed the high potential for a speleothem-based integrated multi-parameter approach for climate reconstruction. The similarity in the climate

response between the growth rate and $\delta^{18}O$ variables of the stalagmites under the NJ-1 and NJ-1202 drip sites showed a greater potential of achieving high-resolution and fast-response climate records than that of stalagmite under the NJ-1203 drip site and provided a possible integration of multiple parameters at a high temporal resolution. The combination of a high rate of modern aragonite deposition, rapid response to seasonal climate of drip water flow rate, and clear and consistent seasonal trends of $\delta^{18}O_{DW}$ and $\delta^{18}O_{aragonite}$ precipitates indicated that stalagmite NJ-1 best preserves the intraseasonal climate variability. The minimum of stalagmite $\delta^{18}O$, which is associated with the maximum growth rate, indicated more rainfall in the late monsoon season (ASO rainfall) or a strong TM. Comparisons with other stalagmite samples and/or other proxies are required to further verify the NJ-1 climatic signals. The $\delta^{18}O$ values and growth rates of the stalagmite under the NJ-1202 drip site can be combined as both proxy indicators of late monsoon rainfall and total rainfall. Tree rings and stalagmites in this area have high potential for multi-proxy comparisons because both natural proxies successfully record paleoseasonality (Cai et al. 2010; Muangsong et al. 2011, 2014, 2016, 2018). Combinations of different parameters and proxies from this area provide the potential for further developing multi-proxy climate reconstructions over different time scales.

6 Conclusion

We present new data on the oxygen isotopic compositions in rainfall, drip water, and their carbonate deposition, as well as the carbonate precipitation amount from the NJ cave in MHS province of NW Thailand based on cave and climate monitoring data collected between August 2012 and October 2013. The data provide the first results of the constraining factors that affect Thai stalagmite parameters and demonstrate the potential use of stalagmites for multi-proxy reconstruction of the Thailand summer monsoon. The conclusions of this study can be summarized as follows:

(1) The $\delta^{18}O_{Rain}$ value from this area reveals a clear similar seasonal pattern, with more enriched $\delta^{18}O_{Rain}$ values during the early rainy season and more depleted $\delta^{18}O_{Rain}$ values during the late rainy season. This seasonal pattern is similar to that of the broad region of Southeast Asia. The shift of $\delta^{18}O_{Rain}$ values possibly results from the domain sources of moisture where an air mass originates.

(2) The $\delta^{18}O_{DW}$ value in the late rainy season is close to the weighted average value of rainfall and is homogenic among monitor drip sites, while those in the dry season are rich in $\delta^{18}O_{DW}$ value due to the evaporation effect in cave, resulting in much heavier and more heterogeneous values among the drip sites. The $\delta^{18}O_{DW}$ value in the early rainy season is influenced by a heavier $\delta^{18}O_{Rain}$ input and

superimposed with evaporation effect, resulting in heavier values compared with those of the late rainy season and exhibiting a discernable season pattern with much heavier values in the dry and early rainy seasons, with more negative values in the late rainy season, especially in September (might also be in late August).

(3) The $\delta^{18}O_{DW}$ value as well as modern $\delta^{18}O_{aragonite}$ precipitated on glass plates generally precipitated at the oxygen isotopic equilibrium during the rainy season, especially in the late rainy season. The dynamic isotope fractionation effect was found to occur in the dry season for site NJ-1, resulting in a small positive excursion that overlapped with the positive $\delta^{18}O_{Rain}$ in the early rainy season, strengthening the seasonal pattern of $\delta^{18}O_{aragonite}$. Because of the greater carbonate deposition in late rainy season for sites NJ-1 and NJ-1202, their $\delta^{18}O_{aragonite}$ response dominates rainfall in the late rainy season, especially in September.

(4) The individual drip rate abruptly increases from September to October, exhibiting a strong response to rainfall in the late rainy season. Seasonal visibilities in the amount of carbonate precipitation show two inverse response patterns to the drip rate. For drip sites in a relatively open environment, e.g., drips NJ-1 and NJ-1202, a strong positive relationship was found between the carbonate deposition amount and feeding drip rate, indicating that the growth rate of the stalagmites fed by these drips was dominated by rainfall during the late rainy season.

(5) Combinations of different stalagmite parameters from this area provide the potential for further developing multi-proxy climate reconstructions over different time scales.

References

Aggarwal PK, Fröhlich K, Kulkarni KM, Gourcy LL (2004) Stable isotope evidence for moisture sources in the Asian summer monsoon under present and past climate regimes. Geophys Res Lett 31: L08203. https://doi.org/10.1029/2004GL019911

Araguás-Araguás L, Froehlich K, Rozanski K (1998) Stable isotope composition of precipitation over Southeast Asia. J Geophys Res Atmos 103:28721–28742. https://doi.org/10.1029/98JD02582

Baker A, Barnes WL, Smart PL (1997) Variations in the discharge and organic matter content of stalagmite drip waters in Lower Cave, Bristol. Hydrol Process 11:1541–1555. https://doi.org/10.1002/(SICI)1099-1085(199709)11:11%3C1541::AID-HYP484%3E3.0.CO;2-Z

Baker A, Asrat A, Fairchild IJ, Leng MJ, Wynn PM, Bryant C, Genty D, Umer M (2007) Analysis of the climate signal contained within δ^{18}O and growth rate parameters in two Ethiopian stalagmites. Geochim Cosmochim Acta 71:2975–2988. https://doi.org/10.1016/j.gca.2007.03.029

Bershaw J (2018) Controls on deuterium excess across Asia. Geosci 8:1–11. https://doi.org/10.3390/geosciences8070257

Buajan S, Pumijumnong N, Li Q, Liu Y (2016) Oxygen isotope (δ^{18}O) of teak tree-ring in northwest Thailand. J Trop For Sci 28:396–405

Buckley B, Palakit K, Duangsathaporn K, Sanguantham P, Prasomsin P (2007) Decadal scale droughts over northwestern Thailand over the past 448 years: links to the tropical Pacific and Indian Ocean sectors. Clim Dyn 29:63–71. https://doi.org/10.1007/s00382-007-0225-1

Cai B, Pumijumnong N, Tan M, Muangsong C, Kong X, Jiang X, Nan S (2010) Effects of intraseasonal variation of summer monsoon rainfall on stable isotope and growth rate of a stalagmite from northwestern Thailand. J Geophys Res Atmos 115:D21104. https://doi.org/10.1029/2009JD013378

Cai B, Zhu J, Ban F, Tan M (2011) Intra-annual variation of the calcite deposition rate of drip water in Shihua Cave, Beijing, China and its implications for palaeoclimatic reconstructions. Boreas 40:525–535. https://doi.org/10.1111/j.1502-3885.2010.00201.x

Chawchai S, Liu G, Bissen R, Jankham K, Paisonjumlongsri W, Kanjanapayont P, Chutakositkanon V, Choowong M, Pailoplee S, Wang X (2018) Stalagmites from western Thailand: preliminary investigations and challenges for palaeoenvironmental research. Boreas 47:367–376. https://doi.org/10.1111/bor.12299

Clark I, Fritz P (1997) Tracing the hydrological cycle. In: Clark I, Fritz P (eds) Environmental isotopes in hydrogeology, Lewis Publishers, pp. 35–61

Cobb KM, Adkins JF, Partin JW, Clark B (2007) Regional-scale climate influences on temporal variations of rainwater and cave dripwater oxygen isotopes in northern Borneo. Earth Planet Sci Lett 263:207–220. https://doi.org/10.1016/j.epsl.2007.08.024

Coplen TB, Hopple JA, Böhlke JK, Peiser HS, Rieder SE, Krouse HR, Rosman KJR, Ding T, Vocke RD, Revesz KM, Lamberty A, Taylor P, De Bièvre P (2002) Compilation of minimum and maximum isotope ratios of selected elements in naturally occurring terrestrial materials and reagents, U.S. Geological Survey Water-Resources Investigations Report 01-4222, pp 98

Dansgaard W (1964) Stable isotopes in precipitation. Tellus A 16:436–468. https://doi.org/10.1111/j.2153-3490.1964.tb00181.x

Denniston RF, Wyrwoll KH, Polyak VJ, Brown JR, Asmerom Y, Wanamaker AD et al (2013) A stalagmite record of Holocene Indonesian–Australian summer monsoon variability from the Australian tropics. Quat Sci Rev 78:155–168. https://doi.org/10.1016/j.quascirev.2013.08.004

Duan W, Cai B, Tan M, Liu H, Zhang Y (2011) The growth mechanism of the aragonitic stalagmite laminae from Yunnan Xianren Cave, SW China revealed by cave monitoring. Boreas 41:113–123. https://doi.org/10.1111/j.1502-3885.2011.00226.x

Duan W, Ruan J, Luo W, Li T, Tian L, Zeng G, Zhang D, Bai Y, Li J, Tao T, Zhang P, Baker A, Tan M (2016) The transfer of seasonal isotopic variability between precipitation and drip water at eight caves in the monsoon regions of China. Geochim Cosmochim Acta 183:250–266. https://doi.org/10.1016/j.gca.2016.03.037

Fairchild IJ, Smith CL, Baker A, Fuller L, Spötl C, Mattey D, McDermott F, EIMF (2006) Modification and preservation of environmental signals in speleothems. Earth Sci Rev 75:105–153. https://doi.org/10.1016/j.earscirev.2005.08.003

Fischer MJ, Treble PC (2008) Calibrating climate-δ^{18}O regression models for the interpretation of high-resolution speleothem δ^{18}O time series. J Geophys Res Atmos 113:D17103. https://doi.org/10.1029/2007JD009694

Fröhlich K, Gibson JJ, Aggarwal PK (2002) Deuterium excess in precipitation and its climatological significance. Proceedings of Study of Environmental Change Using Isotope Techniques. IAEA, IAEA-CSP-13/P, pp 54-66

Genty D, Baker A, Vokal B (2001) Intra- and inter-annual growth rate of modern stalagmites. Chem Geol 176:191–212. https://doi.org/10.1016/S0009-2541(00)00399-5

Hendy CH (1971) The isotopic geochemistry of speleothems—I. The calculation of the effects of different modes of formation on the isotopic composition of speleothems and their applicability as palaeoclimatic indicators. Geochim Cosmochim Acta 35:801–824. https://doi.org/10.1016/0016-7037(71)90127-X

Hondula DM, Sitka L, Davis RE, Knight DB, Gawtry SD, Lee T, Deaton ML et al (2010) A back-trajectory and air mass climatology for the Northern Shenandoah Valley, USA. Int J Climatol 30:569–581. https://doi.org/10.1002/joc.1896

IAEA/WMO (2001) Global network of isotopes in precipitation. The GNIP Database. http://www-naweb.iaea.org/napc/ih/IHS_resources_gnip.html. Accessed 10 November 2016

Kim ST, O'Neil JR, Hillaire-Marcel C, Mucci A (2007) Oxygen isotope fractionation between synthetic aragonite and water: influence of temperature and Mg2+ concentration. Geochim Cosmochim Acta 71:4704–4715. https://doi.org/10.1016/j.gca.2007.04.019

Kuenzer C (2014) Remote sensing the Mekong. Int J Remote Sens 35:2747–2751. https://doi.org/10.1080/01431161.2014.890377

Kumar B, Rai SP, Kumar US, Verma SK, Garg P, Kumar SVV, Jaiswal R, Purendra BK, Kumar SR, Pande NG (2010) Isotopic characteristics of Indian precipitation. Water Resour Res 46:W12548. https://doi.org/10.1029/2009WR008532

Lachniet MS (2009) Climatic and environmental controls on speleothem oxygen-isotope values. Quat Sci Rev 28:412–432. https://doi.org/10.1016/j.quascirev.2008.10.021

Le Duy N, Heidbüchel I, Meyer H, Merz B, Apel H (2018) What controls the stable isotope composition of precipitation in the Mekong Delta? A model-based statistical approach. Hydrol Earth Syst Sci 22:1239–1262. https://doi.org/10.5194/hess-22-1239-2018

Lewis SC, LeGrande AN, Kelley M, Schmidt GA (2010) Water vapour source impacts on oxygen isotope variability in tropical precipitation during Heinrich events. Clim Past 6:325–343. https://doi.org/10.5194/cp-6-325-2010

Lewis SC, Gagan MK, Ayliffe LK, Zhao JX, Hantoro WS, Treble PC, Hellstrom JC, LeGrande AN, Kelley M, Schmidt GA, Suwargadi BW (2011) High-resolution stalagmite reconstructions of Australian–Indonesian monsoon rainfall variability during Heinrich stadial 3 and Greenland interstadial 4. Earth Planet Sci Lett 303:133–142. https://doi.org/10.1016/j.epsl.2010.12.048

Li B, Nychka DW, Ammann CM (2010) The value of multiproxy reconstruction of past climate. J Am Stat Assoc 105:883–895. https://doi.org/10.1198/jasa.2010.ap09379

Li TY, Shen CC, Li HC, Li JY, Chiang HW, Song SR, Yuan DX, Lin CDJ, Gao P, Zhou L, Wang JL, Ye MY, Tang LL, Xie SY (2011) Oxygen and carbon isotopic systematics of aragonite speleothems and water in Furong Cave, Chongqing, China. Geochim Cosmochim Acta 75:4140–4156. https://doi.org/10.1016/j.gca.2011.04.003

Muangsong C, Pumijumnong N, Cai B, Tan M (2011) Stalagmite grey level as a proxy of the palaeoclimate in northwestern Thailand. ScienceAsia 37:262–267. https://doi.org/10.2306/scienceasia1513-1874.2011.37.262

Muangsong C, Cai B, Pumijumnong N, Hu C, Cheng H (2014) An annually laminated stalagmite record of the changes in Thailand monsoon rainfall over the past 387 years and its relationship to

IOD and ENSO. Quat Int 349:90–97. https://doi.org/10.1016/j.quaint.2014.08.037

Muangsong C, Cai B, Pumijumnong N, Hu C, Lei G (2016) Intra-seasonal variability of teak tree-ring cellulose δ^{18}O from northwestern Thailand: a potential proxy of Thailand summer monsoon rainfall. Holocene 26:1397–1405. https://doi.org/10.1177/2F0959683616640045

Muangsong C, Cai B, Pumijumnong N, Lei G, Wang F (2018) A preliminary study on teak tree ring cellulose δ^{18}O from northwestern Thailand: the potential for developing multiproxy records of Thailand summer monsoon variability. Theor Appl Climatol NA 136:1–12. https://doi.org/10.1007/s00704-018-2499-0

Muangsong C, Pumijumnong N, Cai B, Buajan S, Lei G, Wang F, Li M, Payomrat P (2020) Effect of changes in precipitation amounts and moisture sources on inter- and intra-annual stable oxygen isotope ratios (δ^{18}O) of teak trees from northern Thailand. Agric For Meteorol 281:107820

Patterson WP, Smith GR, Lohmann KC (1993) Continental paleothermometry and seasonality using the isotopic composition of aragonitic otoliths of freshwater fishes. In: Swart PK, Lohmann KC, Mckenzie J, Savin S (eds) Climate Change in Continental Isotopic Records, American Geophysical Union, pp. 191-202.

Payomrat P, Liu Y, Pumijumnong N, Li Q, Song H (2018) Tree-ring stable carbon isotope-based June–September maximum temperature reconstruction since AD 1788, north-west Thailand. Tellus Ser B Chem Phys Meteorol 70:1–13. https://doi.org/10.1080/16000889.2018.1443655

Phutong P (2008) Mineralogy and isotope geochemistry of stalagmites in Namjang cave, Pangmapha, Maehongson province, Thailand. Master thesis, Mahidol University.

Pu J, Wang A, Shen L, Yin J, Yuan D, Zhao H (2016) Factors controlling the growth rate, carbon and oxygen isotope variation in modern calcite precipitation in a subtropical cave, Southwest China. J Asian Earth Sci 119:167–178. https://doi.org/10.1016/j.jseaes.2015.12.010

Pumijumnong N, Eckstein D (2011) Reconstruction of pre-monsoon weather conditions in northwestern Thailand from the tree-ring widths of *Pinus merkusii* and *Pinus kesiya*. Trees 25:125–132. https://doi.org/10.1007/s00468-010-0528-4

Pumijumnong N, Muangsong C, Buajan S, Sano M, Nakatsuka T (2020) Climate variability over the past 100 years in Myanmar derived from tree-ring stable oxygen isotope variations in Teak. Theor Appl Climatol 139:1401–1414

Rozanski K, Araguás-Araguás L, Gonfiantini R (1993) Isotopic patterns in modern global precipitation. In: Swart PK, Lohmann KC, Mckenzie J, Savin S (eds) Climate Change in Continental Isotopic Records. American Geophysical Union, pp 1–36

Ryoo JM, Waliser DE, Fetzer EJ (2011) Trajectory analysis on the origin of air mass and moisture associated with atmospheric rivers over the west coast of the United States. Atmos Chem Phys 2011:11109–11142. https://doi.org/10.5194/acpd-11-11109-2011

Sengupta S, Sarkar A (2006) Stable isotope evidence of dual (Arabian Sea and Bay of Bengal) vapour sources in monsoonal precipitation over North India. Earth Planet Sci Lett 250:511–521. https://doi.org/10.1016/j.epsl.2006.08.011

Smith CL, Baker A, Fairchild IJ, Frisia S, Borsato A (2006) Reconstructing hemispheric-scale climates from multiple stalagmite records. Int J Climatol 26:1417–1424. https://doi.org/10.1002/joc.1329

Srivastava R, Ramesh R, Gandhi N, Jani RA, Singh AK (2015) Monsoon onset signal in the stable oxygen and hydrogen isotope ratios of monsoon vapor. Atmos Environ 108:117–124. https://doi.org/10.1016/j.atmosenv.2015.02.062

Stein AF, Draxler RR, Rolph GD, Stunder BJB, Cohen MD, Ngan F (2015) NOAA's HYSPLIT atmospheric transport and dispersion modeling system. Bull Am Meteorol Soc 96:2059–2077. https://doi.org/10.1175/BAMS-D-14-00110.1

Thail Meteorological Department (2013) Average rainfall and temperature data from Mae Hong Son station. http://www.tmd.go.th. Accessed 11 December 2013

Wang B, Ho L (2002) Rainy season of the Asian-Pacific summer monsoon. J Clim 15:386–398. https://doi.org/10.1175/1520-0442(2002)015%3C0386:RSOTAP%3E2.0.CO;2

Wang F, Sun Q, Cai B, Zhang L, Li M, Li T (2016) Variation of δ^{18}O in the meteoric precipitation, drip water and their calcite deposition in Miaodong Cave, Liaoning Province and its implications for palaeoclimatic reconstructions. J Quat Sci 36:1370–1382

Wei Z, Lee X, Liu Z, Seeboonruang U, Koike M, Yoshimura K (2018) Influences of large-scale convection and moisture source on monthly precipitation isotope ratios observed in Thailand, Southeast Asia. EPSL 488:181–192. https://doi.org/10.1016/j.epsl.2018.02.015

West JB, Bowen GJ, Cerling TE, Ehleringer JR (2006) Stable isotopes as one of nature's ecological recorders. Trends Ecol Evol 21:408–414. https://doi.org/10.1016/j.tree.2006.04.002

Yadava GM, Ramesh R, Pant BG (2004) Past monsoon rainfall variations in peninsular India recorded in a 331-year-old speleothem. Holocene 14:517–524. https://doi.org/10.1191/0959683604hl728rp